Technical Report

TR-99-21

Experimental and modeling study of the interaction between Uranium (VI) and magnetite

Fatima El Aamrani, Ignasi Casas and Joan de Pablo
Chemical Engineering Department,
Universitat Politècnica Catalunya, Barcelona, Spain

Lara Duro, Mireia Grivé and Jordi Bruno
QuantiSci S L Parc Tecnològic del Vallès,
Cerdanyola del Vallès, Spain

Svensk Kärnbränslehantering AB

October 1999

Svensk Kärnbränslehantering AB
Swedish Nuclear Fuel
and Waste Management Co
Box 5864
SE-102 40 Stockholm Sweden
Tel 08-459 84 00
+46 8 459 84 00
Fax 08-661 57 19
+46 8 661 57 19

Experimental and modeling study of the interaction between Uranium (VI) and magnetite

Fatima El Aamrani, Ignasi Casas and Joan de Pablo
Chemical Engineering Department,
Universitat Politècnica Catalunya, Barcelona, Spain

Lara Duro, Mireia Grivé and Jordi Bruno
QuantiSci S L Parc Tecnològic del Vallès,
Cerdanyola del Vallès, Spain

Svensk Kärnbränslehantering AB

October 1999

Abstract

We have studied the interaction of U(VI) with the surface of synthetic magnetite by means of solution and solid techniques (X-Ray Photoelectron Spectroscopy). The experimental program has focused on the study of this interaction at the pH of interest under granitic groundwater (8-9) in solutions containing total carbonate concentrations in the range 10^{-4} to 10^{-3} mol/dm^3. An increase of the uptake of uranium is observed with low carbonate concentrations in solution. The interaction has been studied as a function of the total uranium concentration and the solid surface area/solution volume ratio. The attachment of uranium to the surface of the solid can be explained in terms of a non-electrostatic surface complexation model involving two different surface complexes: >FeO-UO_2^+ and >FeO-$UO_2(OH)_2^-$. The XPS study indicates the possibility reduction of U(VI) on the surface of magnetite to U(IV) due to the electronic transference between Fe and U, causing the oxidation of Fe(II) to Fe(III).

Table of contents

1 Introduction

Magnetite has been identified as a corrosion product of carbon steel canister in closed experiments with initial low oxygen content at temperatures between 90ºC and 170ºC /Smailos et al, 1992/. Under these conditions, iron corrodes to produce $Fe(OH)_2(s)$, in the so-called Schikorr reaction:

$$Fe(s) + H_2O = Fe(OH)_2\ (s) + H_2(g)$$

The oxidation of the iron(II) hydroxide produces a protective passive oxide layer. The composition of this layer is not known but it has been suggested that it consists of an oxide $Fe_{3-x}O_4$ with a spinel structure varying in composition from Fe_3O_4 (magnetite), in oxygen-free solutions, to $Fe_{2.67}O_4$ under the presence of oxygen /Stumm and Morgan, 1996/.

The global redox reaction of transformation of iron into magnetite under anoxic conditions can be written as follows:

$$3\ Fe\ (s) + 4\ H_2O = Fe_3O_4\ (s) + 4\ H_2(g)$$

Recently, White and Peterson /1996/ have demonstrated that structural Fe(II) in magnetite is able to heterogeneously reduce ferric, cupric, vanadate and chromate ions at the oxide surfaces over a pH range of 1-7 at 25ºC. For an aqueous transition metal M, the following process can be written:

$$3\{Fe^{2+}Fe^{3+}\}O_4\ (s) + 2/n\ M^z = 4\ \{Fe_2^{\ 3+}\}O_3 + Fe^{2+} + 2/n\ M^{z-n}$$

where z is the valence state and n is the charge transfer number. The authors pointed out that the half-cell potential range for solid state oxidation {Fe(II)} → {Fe(III)} ranges from –0.34 to –0.65 V, making structural Fe(II) a stronger reducing agent than aqueous Fe^{2+} (-0.77 V).

The reduction process of Tc(VII) and Np(V) by aqueous Fe^{2+} and magnetite has also studied /Cui and Eriksen, 1996/. Magnetite seemed to be an effective reductant for TcO_4^- while a simple sorption process was able to explain the experimental results obtained when using Np(V). Fujita et al /1995/ reached similar conclusions for Np(V).

Results of uranium/magnetite interaction found in the literature are scarce. Grambow et al /1996/ studied the sorption and subsequent reduction of U(VI) onto canister corrosion products (iron(II) hydroxide and magnetite) and observed that the reduction of U(VI) to U(IV) was lower than expected. El Aamrani et al /1998/ have shown a decrease of the U(VI) aqueous concentration in the presence of magnetite but the authors did not identify the process responsible of this decrease. Finally, Sagert and Ho /1989/ observed that the sorption of U(VI) onto magnetite in carbonate medium is similar to the one obtained in the presence of hematite.

X-ray Photoelectron Spectroscopy (XPS) is a surface-sensitive technique (i.e. analysis depth ≈ 10 nm) whose strength lies in its ability to determine the various chemical redox states of a given surface species. This technique has been used to study the surface of different mineral oxides, magnetite among them /Allen et al, 1974a, McIntyre and

Zetaruk, 1977/. The relative concentrations of Fe(II) and Fe(III) on the surface of the solid can be determined by the deconvolution of Fe(3p) peak. There are several studies in the literature dealing with the redox interaction between U(VI) and the surface of minerals. Wersin et al /1994/ studied the interaction between U(VI) and sulphide minerals, Rodriguez et al /1998/ used FeO-rich olivine and Fiedor et al /1998/ zero-valent iron. In some cases, the deconvolution of U (4f) peak allowed to determine the percentage of U(IV) and U(VI) onto the surface /Allen et al, 1974b, Shoesmith et al, 1989, de Pablo et al, 1996/.

In this work, we have studied the uptake of uranium to the surface of magnetite taking into account two processes: 1) sorption of the U(VI) onto the magnetite, this process has been modelled considering a surface complexation mechanism; 2) heterogeneous reduction of U(VI) to U(IV) on the magnetite surface.

2 Experimental procedure

2.1 Magnetite characterisation

The magnetite used in this study was supplied by Aldrich, with a purity of 98% and particle size less than 5 μm. X-Ray Diffractogram showed a small percentage of Iron(III) oxide. Surface area was determined by the BET methodology, the value obtained was 1.58 ± 0.01 $m^2\ g^{-1}$.

2.2 Experimental procedure

Batch experiments to study the uptake of uranium onto the surface of magnetite were conducted at different initial uranium concentrations, different bicarbonate concentrations in solution and different surface area to volume ratio in order to determine the influence of these parameters on the equilibrium reached between the surface of the solid and the contacting solution.

An inert electrolyte, $NaClO_4$, was used to prepare the ionic medium. In all the experiments performed, the contacting solution was prepared in a way that

$$[(Na)HCO_3] + [(Na)ClO_4] = 0.1\ mol \cdot dm^{-3}$$

20 cm^3 of ionic medium were put in contact, at 25°C in stoppered glass tubes, with weighed amounts of magnetite of particle size (dp) < 5 μm. In order to maximise the contact between the solid and the solution, the tubes were continuously shaken in a rotary mixer. After the contacting period, samples of the supernatant solution were withdrawn, filtered through a 0.22 μm pore size SARTORIUS filters and analysed for their uranium content by means of an SCINTREX UA-3 laser fluorimeter.

The analyses of the solution are given in units of moles of uranium per dm^3 of aqueous phase ([U]aq). The concentration of uranium attached to the solid ({U}s) in units of moles of U per g of solid (or per m^2 of solid) is calculated by subtracting [U]aq to the total initial concentration of uranium added to the solution ([U]o) and normalising with the weight to volume (or surface area to volume) ratio:

$$\{U\}s = ([U]o - [U]aq) \times (V/w);$$

V in dm^3 and w in g.

2.3 Kinetic tests

A preliminary series of experiments were conducted to establish the time needed for the system to reach equilibrium. The experimental conditions of these tests (kinetic tests) are shown in Tables 2-1 and 2-2.

Table 2-1. Kinetic tests A. 20 cm³ of the ionic media in contact with 1 g of magnetite and in contact with air.

Kinetic test	$[HCO_3^-]o$ (mol·dm^{-3})	[U]o (mol·dm^{-3})	initial pH
KTA.1	0	$5 \cdot 10^{-7}$	8.8
KTA.2	10^{-4}	$7.96 \cdot 10^{-7}$	8.7
KTA.3	$5 \cdot 10^{-3}$	$9.32 \cdot 10^{-6}$	8.7

Table 2-2. Kinetic tests B. 20 cm³ of the ionic media in contact with 1 g of magnetite and a continuous bubbling of N_2(g).

Kinetic test	$[HCO_3^-]o$ (mol·dm^{-3})	[U]o (mol·dm^{-3})	initial pH
KTB.1	10^{-4}	$3.05 \cdot 10^{-6}$	8.7
KTB.2	$4 \cdot 10^{-4}$	$8.47 \cdot 10^{-6}$	8.8
KTB.3	10^{-3}	$8.65 \cdot 10^{-6}$	8.7

2.4 Equilibrium tests (ET)

After establishing the time needed for the system to reach equilibrium, 5 different series of equilibrium tests were performed. All of them were in contact with air and at pH = 8.7 (see Table 2-3).

Table 2-3. Equilibrium tests. 20 cm³ of the ionic media in contact with magnetite and in contact with air.

Experiment	$[HCO_3^-]o$ mol·dm^{-3})	[U]o (mol·dm^{-3})	w (g)
ETI	10^{-4}	$3.05 \cdot 10^{-6}$	0.1 to 2
ETII	$4 \cdot 10^{-4}$	$8.47 \cdot 10^{-6}$	"
ETIII	10^{-3}	$8.65 \cdot 10^{-6}$	"
ETIV	10^{-4}	$9.41 \cdot 10^{-6}$	"
ETVa	$4 \cdot 10^{-4}$	$1.8 \cdot 10^{-7}$ to $8.5 \cdot 10^{-6}$	1
ETVb	"	"	0.2
ETVc	"	"	0.1

2.5 X-ray Photoelectron Spectroscopy Tests (XPS)

Magnetite was examined by XPS before and after uranium(VI) attachment. Spectra were recorded on a PHI Perkin Elmer ESCA Multianalyzer 5500 using an Al-K_α X-ray source (1486.6 eV). The error in the determination of the electron energies was ± 0.2 eV.

The results obtained previously to the interaction with uranium have been analysed according to the study reported by McIntyre and Zetaruk /1977/ and the uranium results as in a previous work using the same ESCA Multianalyzer /Rodriguez et al,1998/. The experimental conditions are collected in Table 2-4.

Table 2-4. XPS tests. Experimental conditions.

Experiment	Conditions	[U]o ($mol \cdot dm^{-3}$)	Magnetite (g)
XPI			Initial
XPII dissolution	$[HCO_3^-]=10^{-4}$ M, N_2, t=2 days	–	1
XPIII dissolution	pH=5.6, O_2 t=2 days	–	1
XPIV dissolution	pH=3, N_2 t=2 days	–	1
XPUI	pH=4.8, N_2, t=57, 85 days	$1.6 \cdot 10^{-4}$	1
XPUII	$[HCO_3^-]=2.4 \cdot 10^{-3}$ M N_2, t=1,120,150 days	$1.3 \cdot 10^{-4}$	2.9
XPUIII	$[HCO_3^-]=10^{-4}$ M, N_2 t=days	10^{-6}	1

3 Results of U(VI)/magnetite interaction

In this section, the results obtained from the experiments are presented and modelled.

3.1 Contact time needed to reach equilibrium (results from KT)

The time needed for the system to reach equilibrium is shown in Figures 3-1 and 3-2 for the experiments performed in contact with air and by bubbling $N_2(g)$ through the solution.

From these figures we can observe that the time needed for the system to reach equilibrium is larger in the case of the experiments performed by bubbling $N_2(g)$ through the solution. In contact with air, the equilibration time is lower than 4 hours, while under anoxic conditions it takes between 100 and 200 h. to reach equilibrium. It is also worthy to note that the presence of carbonate affects the behaviour of uranium to a large extent, decreasing the uranium uptake by the solid.

From these results, we selected an equilibrium time for the equilibrium tests in oxic conditions of 4 h.

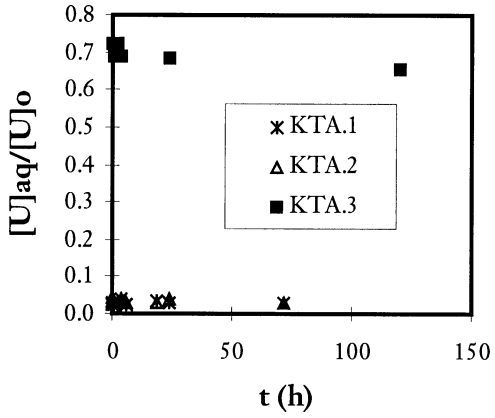

Figure 3-1. *Evolution of the ratio [U]aq/[U]o with time in the kinetic experiments performed in contact with air (KTA).*

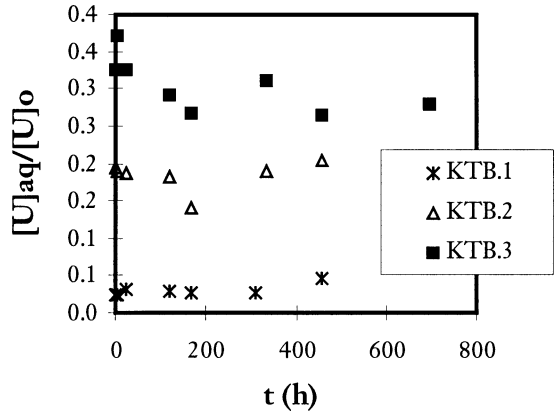

Figure 3-2*. Evolution of the ratio [U]aq/[U]o with time in the kinetic experiments performed in contact with $N_2(g)$ (KTB).*

3.2 Results from equilibrium tests (ET)

The results obtained from the different series of equilibrium tests are shown in Table 3-1.

Table 3-1. Results obtained from the equilibrium experiments.

Test	[U]o (mol/dm³)	[HCO_3^-] (mol/dm³)	w(g)	[U]aq (mol/dm³)	{U}s (mol/g)
ETI	3.05E-06	1e-04	1	1.15E-07	5.87E-08
	3.05E-06	1e-04	1.5	7.76E-08	3.96E-08
	3.05E-06	1e-04	2	7.76E-08	2.97E-08
ETII	8.47E-06	4e-04	0.1	4.58E-06	7.78E-07
	8.47E-06	4e-04	0.5	3.21E-06	2.11E-07
	8.47E-06	4e-04	1	1.83E-06	1.33E-07
	8.47E-06	4e-04	1.5	1.13E-06	9.79E-08
	8.47E-06	4e-04	2	7.94E-07	7.68E-08
ETIII	8.65E-06	1e-03	0.1	6.87E-06	3.55E-07
	8.65E-06	1e-03	0.5	5.35E-06	1.32E-07
	8.65E-06	1e-03	1	3.44E-06	1.04E-07
	8.65E-06	1e-03	1.5	2.29E-06	8.48E-08
	8.65E-06	1e-03	2	1.68E-06	6.97E-08
ETIV	9.41E-06	1e-04	0.1	8.95E-07	1.70E-06
	9.41E-06	1e-04	0.5	3.16E-07	3.64E-07
	9.41E-06	1e-04	1	1.79E-07	1.85E-07
	9.41E-06	1e-04	1.5	1.41E-07	1.24E-07
	9.41E-06	1e-04	2	1.13E-07	9.30E-08
ETVa	8.47E-06	4e-04	1	1.83E-06	1.33E-07
	3.60E-06	4e-04	1	6.16E-07	5.97E-08
	3.49E-06	4e-04	1	5.75E-07	5.83E-08
	7.32E-07	4e-04	1	8.15E-08	1.30E-08
	4.31E-07	4e-04	1	8.54E-08	6.91E-09
	3.71E-07	4e-04	1	6.76E-08	6.07E-09
	3.06E-07	4e-04	1	7.83E-08	4.55E-09
	1.53E-07	4e-04	1	6.40E-08	1.78E-09
ETVb	6.93E-06	4e-04	0.2	3.49E-06	3.44E-07
	5.39E-06	4e-04	0.2	2.85E-06	2.54E-07
	3.83E-06	4e-04	0.2	2.22E-06	1.61E-07
	2.38E-06	4e-04	0.2	1.08E-06	1.30E-07
	7.28E-07	4e-04	0.2	2.34E-07	4.94E-08
	5.15E-07	4e-04	0.2	9.96E-08	4.15E-08
	3.44E-07	4e-04	0.2	7.83E-08	2.66E-08
	1.85E-07	4e-04	0.2	7.11E-08	1.14E-08
ETVc	6.93E-06	4e-04	0.1	5.04E-06	3.78E-07
	5.39E-06	4e-04	0.1	3.81E-06	3.17E-07
	3.83E-06	4e-04	0.1	2.40E-06	2.86E-07
	2.38E-06	4e-04	0.1	1.32E-06	2.12E-07
	7.28E-07	4e-04	0.1	3.72E-07	7.12E-08
	5.15E-07	4e-04	0.1	1.91E-07	6.49E-08
	3.44E-07	4e-04	0.1	1.40E-07	4.07E-08
	1.85E-07	4e-04	0.1	8.03E-08	2.09E-08

In Figure 3-3, the concentration of uranium linked to the solid in units of mol per gram of solid versus the concentration of uranium in solution for the different bicarbonate concentrations tested in this work is shown. As we can see, the slope of the plots is sharper for the lowest bicarbonate concentrations, indicating a larger value of the distribution coefficient (Kd), defined as:

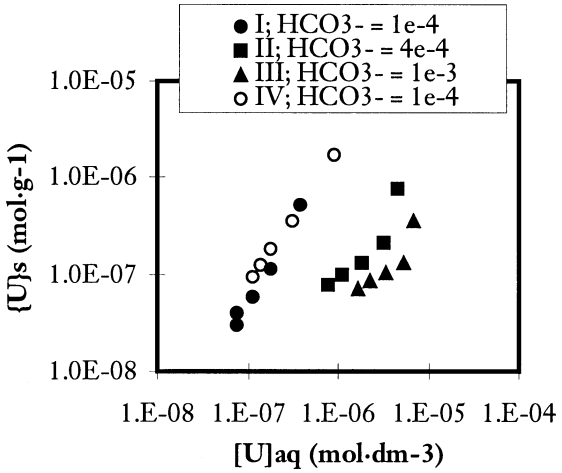

Figure 3-3. *Plot of the concentration of uranium linked to the solid in front of the aqueous concentration of uranium.*

$$Kd = \{U\}s/[U]aq$$

which reflects that the lowest the concentration of bicarbonate in solution, the strongest the interaction between uranium and the surface of the solid, as it is expected according to the very stable aqueous carbonate-U(VI) complexes and it was already observed by Sagert and Ho /1989/.

The different values obtained for the distribution coefficient are shown in Table 3-2 and we can observe the increase of the value of Kd at lower bicarbonate concentration.

Table 3-2. Values of Kd's at different bicarbonate concentration.

Test	$[HCO_3^-]$	Kd(dm^3/g)
ETI	$1.00 \cdot 10^{-4}$	0.64
ETII	$4.00 \cdot 10^{-4}$	0.05
ETIII	$1.00 \cdot 10^{-3}$	0.017
ETIV	$1.00 \cdot 10^{-4}$	1.3

As mentioned in the experimental part, the experiments labelled ETV were performed by varying the concentration of uranium at fixed weight to volume ratios (50, 10 and 5 g/dm^3) and at a fixed bicarbonate concentration of $4 \cdot 10^{-4}$ mol·dm^{-3}. The results obtained, plotted as concentration of uranium linked to the solid versus the total concentration of uranium added to the solution are shown in Figure 3-4. This indicates that no saturation of the surface sites available for the co-ordination of the metal to the surface of the solid is reached, since the slope of the data does not decrease when increasing the value of [U]tot.

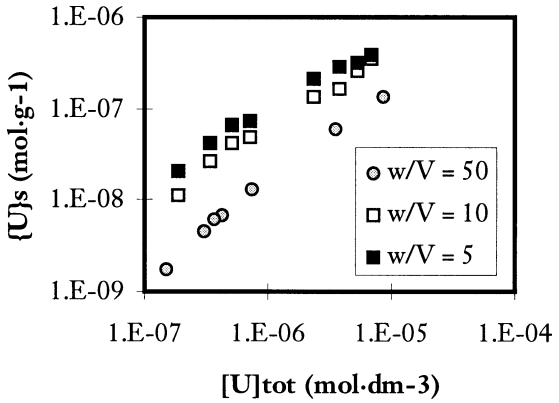

***Figure 3-4**. Plot of concentration of uranium linked to the solid vs. the total concentration of uranium added to the solution at $4 \cdot 10^{-4}$ mol HCO_3^- per dm^3 of solution.*

3.3 Data treatment

The electronic transference between a solid and a solute requires the attachment of the solute to the surface of the solid. For this reason, the first modelling we have conducted aims to understand the equilibrium attained between the surface of the solid and the uranium initially present in solution. For this objective, we have applied a simple surface complexation modelling by neglecting electrostatic factors.

The selection of the parameters needed to conduct this type of modelling is discussed below.

3.3.1 Magnetite surface acidity constants

In order to define our system from a surface co-ordination point of view, the first thing we need to determine is the surface acidity of the solid. We have not run surface titrations to determine the intrinsic acidity constants of the surface of magnetite but we have conducted a literature search in order to ascertain the range of values determined by other authors for these parameters.

Tewari and McLean /1971/ studied the dependence of the point of zero charge (pzc) of magnetite with temperature. They found that the pzc decreased from 6.55 at 25°C to 5.4 at 90°C.

Blesa et al /1983/ studied the dependence of the pzc of magnetite with temperature. Their results are comparable with those obtained by Tewari and McLean /1971/.

Sverjensky and Sahai /1996/ estimated the equilibrium constants for the protonation of the surface of oxides and silicates. They used a combination of the electrostatic theory from Yoon et al, /1979/ and the Born solvation theory. In this way, they related the surface protonation reactions with the Pauling bonding strength and the dielectric constant of the mineral.

Tamura et al /1996/ conducted measurements of the density of surface charge of different minerals (magnetite among them) and found a relationship between the surface charge and pH.

In the following table a summary of the values obtained for K_1 and K_2 in the literature is shown, where:

$$>FeOH_2^+ = >FeOH + H^+; \qquad K_1$$
$$>FeOH = >FeO^- + H^+; \qquad K_2$$

Table 3-3. Surface acidity constants.

ϕ (μm)	SA (m^2g^{-1})	T (°C)	LogK_1	logK_{2-}	pzc	I	Model	Source
		25			6.55			Tewari and McLean /1971/
		90			5.4			
0.22	5.44	25			6.90a	KNO_3	Site Binding Model	Blesa et al /1983/
		30	-4.40	-9.00	6.80			
		50	-4.15	-8.70	6.45			
		80	-3.70	-8.20	6.00			
1.1	3.3	25			6.4	500 mmol/l NaCl		Sagert and Ho /1989/
1.1	3.3	25			6.75	1mmol/l $NaHCO_3$		
		25	-4.9	-9.9	6.95	0.001	Const. capac.	
			-5.4	-9.5	7.4	0.01		
			-5.8	-9.1	7.45	0.1		
		25	-5.9	-9.0	7.5		DDL	Sverjensky and Sahai /1996/
		25	-4.2	-10.0	7.1		TDL	
	4.32	25			6.25	0.1 ($NaNO_3$)		Tamura et al /1996/

From this set of values, we selected for the inclusion in our data treatment a value of $logK_1$ = -5 and $logK_2$ = -10, because of having been obtained at the lowest ionic strength (0.001 M) and by using a constant capacitance model by Sverjensky and Sahai /1996/.

3.3.2 Magnetite surface area and density of surface sites

We have measured the surface area of our magnetite samples by means of BET-N2 and a value of 1.58 ± 0.01 $m^2 \cdot g^{-1}$. has been obtained. This value is somewhat lower than the one found in the literature, /Inagaki et al, 1998/ for a synthetic magnetite of the same particle size than the one used in our experiments: 7.9 $m^2 \cdot g^{-1}$.

For the value of the density of surface sites, we follow the recommendation of Davis and Kent /1990/ and we use a value of 2.31 site$\cdot nm^{-2}$ for magnetite. For explanations on the selection of this value, see the mentioned reference.

By using these values, we obtain the following mass density of surface sites:

$(1.58 m^2/g)$ x $(2.31$ sites$/nm^2)$ x $(10^{18}$ $nm^2/m^2)$ x $(1$ mol sites$/6.023 \cdot 10^{23}$ sites) =
$= 6.06 \cdot 10^{-6}$ mol sites/g solid

In order to see which is the value of surface sites determined from the experimental data we have performed a simple treatment of the series of experiments ETVa, b and c by applying a Langmuir isotherm to the data collected at constant weight of solid.

3.3.3 Langmuir isotherm

The Langmuir isotherm is based on the assumption of a very simple equilibrium established between the surface of the solid, S, and the metal in solution, U, which can be expressed by the following equilibrium and mass action law:

$$S + U = SU;\ K = [SU] / ([S] \cdot [U])$$

In our case, [U] = [U]aq and [SU] = [U]s, all in units of mol of uranium per dm^3 of solution.

On the other hand, we know that the total concentration of surface sites, [S]tot will be the sum of the free surface sites, [S] plus the occupied surface sites ([SU] or [U]s) and therefore:

$$[S]tot = [U]s + [S]$$

and by combining the former equation with the mass action law we obtain the following general expression of the Langmuir isotherm:

$$[U]s = K \cdot [S]tot \cdot [U]aq / (1 + K \cdot [U]aq)$$

which will allow the estimation of [S]tot by adjusting this type of equation to a series of data obtained at constant weigh of solid.

The results of the adjustment of the Langmuir isotherm to the experimental data collected from ETVa, b and c are shown in Table 3-4.

Table 3-4. Results of the Langmuir isotherm adjustment.

Test	K	[S]tot (mol·dm^{-3})	{S}tot (mol·g^{-1})
ETVa	$(3.23 \pm 0.74) \cdot 10^5$	$(1.79 \pm 0.29) \cdot 10^{-5}$	$3.58 \cdot 10^{-7}$
ETVb	$(1.57 \pm 0.38) \cdot 10^6$	$(2.07 \pm 0.19) \cdot 10^{-6}$	$4.94 \cdot 10^{-7}$
ETVc	$(5.54 \pm 0.93) \cdot 10^5$	$(2.47 \pm 0.16) \cdot 10^{-6}$	$2.07 \cdot 10^{-7}$

The comparison between the data and the theoretical fitting from where we obtained the parameters shown in the previous table is shown in Figure 3-5.

We can observe that the line fitted to series ETVb does not reproduce the behaviour of the last two points obtained from these experiments, which can be due to the involvement of different type of sites of the surface.

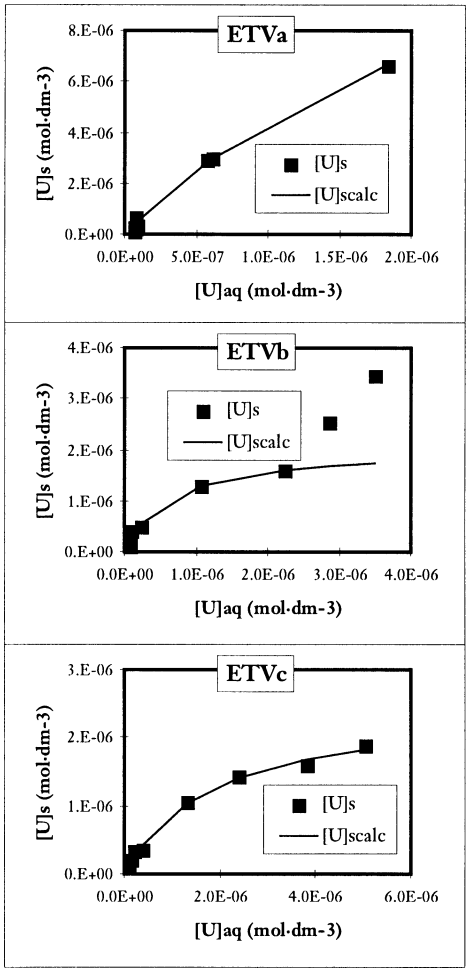

Figure 3-5. *Fitting of a Langmuir isotherm equation to the data gathered from experiments ETVa, b and c.*

We can also see that the different values obtained from the density of surface sites {S}tot, are comparable. Nevertheless, we can also see that these values are one order of magnitude lower than the value calculated by using the surface density proposed by Davis and Kent [1990] and the surface area experimentally determined. By analysing the experimental data plotted in Figures 3-3 and 3-4, we can see that in several cases we have sorbed more uranium than the average value of the density of surface sites determined from the Langmuir analyses and, for this reason, we rather use the value calculated by using the measured BET surface area and the site density proposed by Davis and Kent: $6.06 \cdot 10^{-6}$ mol·g^{-1}

3.3.4 Results of the modelling

We have proposed the following surface complexation equilibria in order to explain the interactions between uranium and the surface of magnetite observed and shown in the previous sections:

$$>FeOH + H^+ = >FeOH_2^+;\ logK_1 = 5 \qquad \text{(eq.1)}$$

$$>FeOH = >FeO^- + H+;\ logK_2 = -10 \qquad \text{(eq.2)}$$

$$>FeOH + UO_2^{2+} = >FeO\text{-}UO_2^+ + H^+ ;\ logK_a \qquad \text{(eq.3)}$$

$$>FeOH + UO_2^{2+} + H_2O = >FeO\text{-}UO_2(OH) + 2\ H^+ ;\ logK_b \qquad \text{(eq.4)}$$

$$>FeOH + UO_2^{2+} + 2\ H_2O = >FeO\text{-}UO_2(OH)_2^- + 3\ H^+ ;\ logK_b \qquad \text{(eq.5)}$$

The values of $\log K_1$ and $\log K_2$ have been taken from the literature, as explained in section 4.1, while the values of K_a, K_b and K_c have been adjusted to the data by means of a minimisation procedure using the Microsoft Origin™ code. The NEA /Grenthe et al, 1992/ thermodynamic database has been used for the aqueous uranium speciation, except for the complex $UO_2(OH)_2(aq)$, for which the value recommended by SKB /Bruno and Puigdomènech, 1989/ has been taken.

In order to simplify the system, we have not included any electrostatic term in the analyses, and we have proposed the simplest surface co-ordination equilibria given by equations 3, 4 and 5.

From the fitting to the data, the following values for K_a and K_b have been obtained:

$$K_a = 139 \pm 0.45$$

$$K_b = 0$$

$$K_c = (2.76 \pm 0.32) \cdot 10^{-15}$$

From these results we can see that two different surface complexes may explain the sorption of uranium onto magnetite under the experimental conditions used in our study: $>FeO\text{-}UO_2^+$ and $>FeO\text{-}UO_2(OH)_2^-$.

The data calculated by using these constants are compared with the experimental data in Figure 3-6.

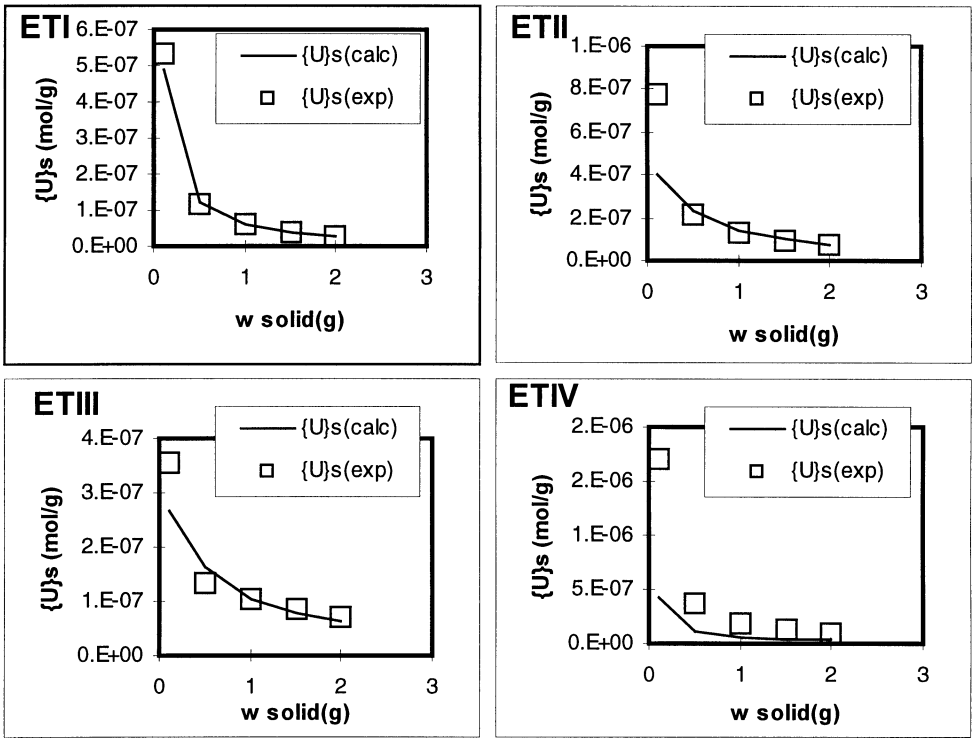

***Figure 3-6**. Comparison between the experimental and the calculated concentration of uranium bound to the solid in ETI to ETIV.*

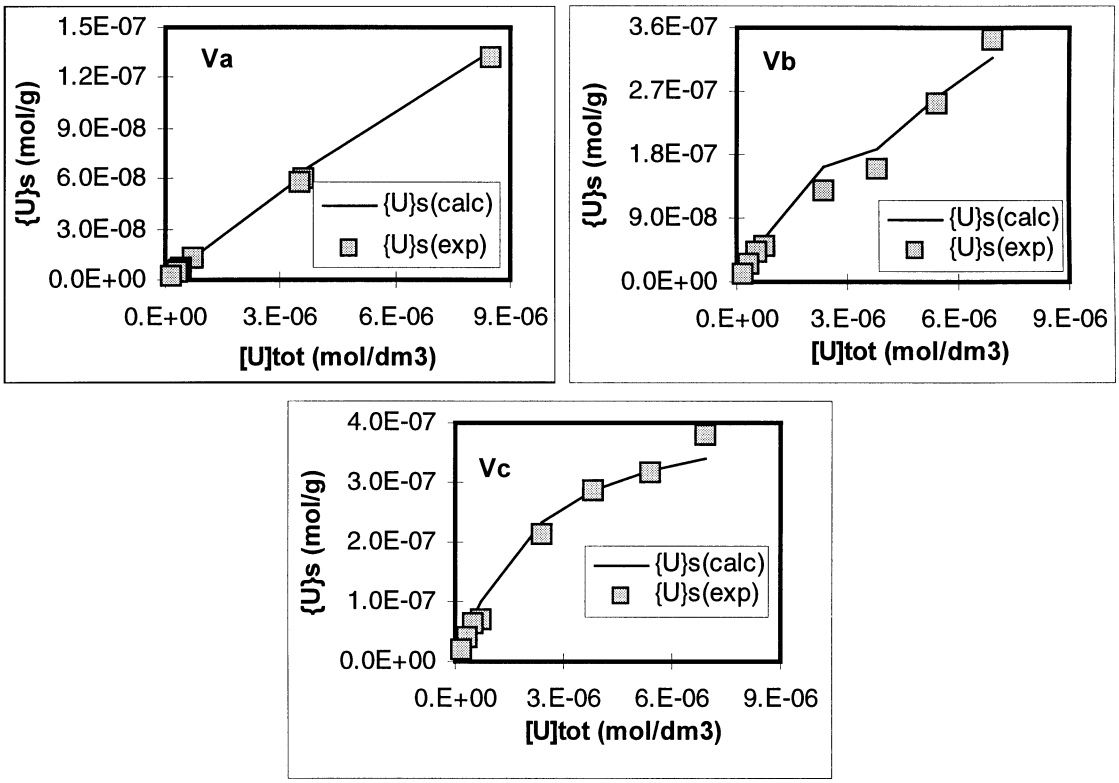

Figure 3-7*. Comparison between the experimental and the calculated concentration of uranium bound to the solid in ETVa to ETVc.*

From the former figure we can see a reasonable agreement between the data and the calculation except for those experiments performed with the lowest weight of solid. In fact, the actual concentration of uranium bound to the solid is larger than the concentration calculated. There may be many different reasons for this discrepancy. When lower amounts of solid are present in the experiment, the contact between solid and solution can be more effective than expected, what would explain this discrepancy.

The same type of comparison is shown in Figure 3-7 for ETVa to ETVc.

From Figure 3-7, we can see a very good agreement between the experimental and the calculated values of uranium co-ordinated to the surface of the solid.

4 Results of XPS study

The deconvolution of the Fe (3p) signal in three different peaks allows to determine the relative concentration of Fe(II) and Fe(III) on the magnetite surface, according to McIntyre and Zetaruk [1977]. The lower binding energy peak represents the Fe(II) contribution while the two peaks at high binding energy indicate the contribution of Fe(III). By applying this treatment to the magnetite samples previously to the addition of uranium, we obtained the Fe(II)/Fe(III) ratios shown in Table 4-1.

Table 4-1. Fe(II)/Fe(III) ratio of magnetite surface.

Experiment	Fe(II)/Fe(III) ratio
XPI	0.49
XPII dissolution	0.51
XPIII dissolution	0.35
XPIV dissolution	0.41

The spectra of the different experiments are shown in Figures 4-1 to 4-4. Untreated commercial magnetite (XPI) shows an excellent agreement with the theoretical ferrous/ferric stoichiometry of 0.5 in Fe_3O_4. We can see that the ratio Fe(II)/Fe(III) in experiment XPII is very similar to the one of pure magnetite, which is probably due to the presence of bicarbonate in solution. On the other hand, the presence of oxygen in XPIII produces an increase in the relative concentration of Fe(III), as it was expected and already reported by in White /1990/. In acidic medium (XPIV), the Fe(II)/Fe(III) also decreases which has been interpreted by Jolivet and Tronc /1988/ as a preferential release of Fe(II) with respect to Fe(III), and not to an increase in the oxidation of the initial Fe(II) present on the surface.

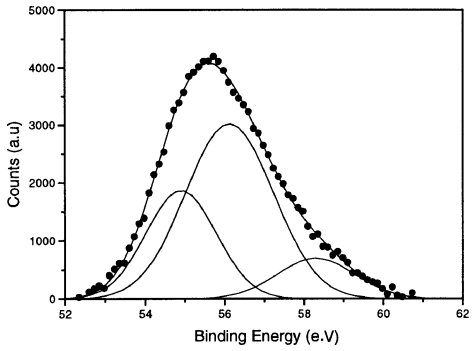

Figure 4-1. *Fe(3p) peak for commercial F_3O_4.*

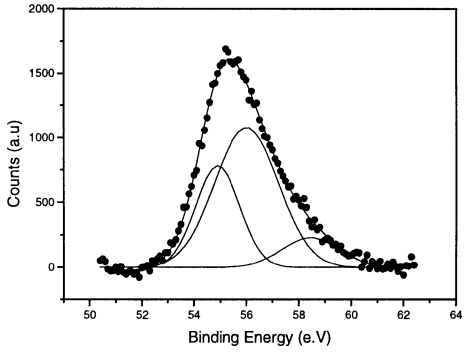

Figure 4-2. *Fe(3p) peak in experiment XPUII.*

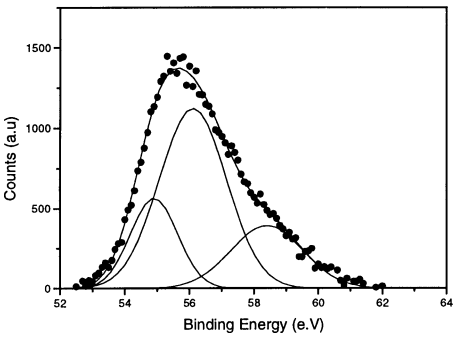

***Figure 4-3**. Fe(3p) peak in experiment XPUIII.*

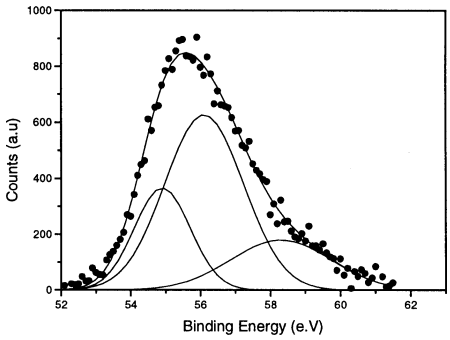

***Figure 4-4**. Fe(3p) peak in experiment XPUIV.*

The XPS results obtained form the experiments where uranium was added to the solution in contact with magnetite are collected in the Table 4-2.

Table 4-2. XPS results in the uranium(VI)/magnetite interaction experiments.

Experiment	Time (days)	Fe(II)/Fe(III) ratio	Energy binding of U4f peak
XPUI	57	0.22	382.0
	85	0.15	382.0
XPUII	1	–	382.0
	120	0.45	381.7
	150	0.46	381.8
XPUIII	120	0.40	381.9

The U 4f peak in the XPUI experiment after 85 days is shown in Figure 4-5, the peak maximum is at 382.0 eV which indicates no reduction of the U(VI) at these conditions. The low Fe(II)/Fe(III) ratio is attributed to the preferential Fe^{2+} release at acid pH commented above. This Fe^{2+} release could imply a decrease of the reduction capacity of the magnetite.

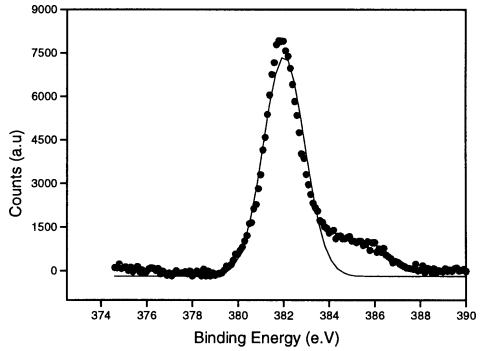

***Figure 4-5**. U(4f) peak in experiment XPUI after 85 days.*

In experiment XPUII, a small shift of the maximum energy binding (from 382.0 to 381.7) was observed after 120 and 150 days. This shift can be attributed to the reduction of U(VI) on the magnetite surface since this effect was not observed after 1 day. Similar shifts were observed by Wersin et al /1994/ using galena and pyrite but after only in 6–8 days of contact between the solid and the uranium solution. This finding would indicate a higher reduction capacity of these sulphide minerals compared to magnetite. In Figure 4-6, we can compare the uranium 4f peak obtained from experiment XPUII after 1 and 120 days of contact.

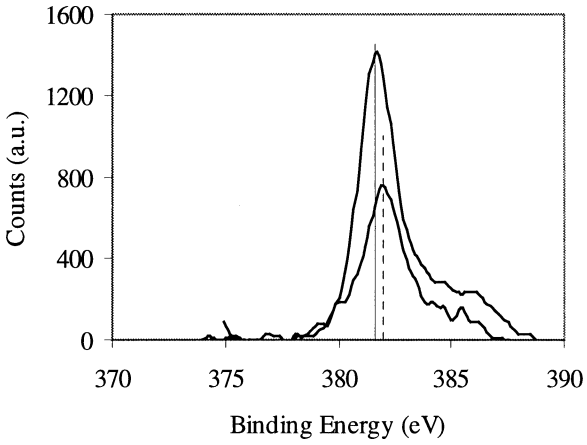

Figure 4-6. *U(4f) peak in the experiment XPUII. Peak maximum 382.0 after 1 day; 381.7 after 120 days.*

5 Conclusions

The electron transference between the surface of magnetite and aqueous U(VI) must be preceded by the attachment of U(VI) to the surface of the solid.

This process of binding or sorption of U(VI) to the magnetite surface is relatively fast and reaches equilibrium in about 4 hours when the system is under oxic conditions. When anoxic conditions are maintained by means of a continuous $N_2(g)$ bubbling, the time to reach equilibrium increases up to 200 hours.

The sorption extent is decreased in the presence of carbonate in solution, due to the formation of very stable aqueous U(VI)-carbonate complexes. Under the typical carbonate concentrations of granitic groundwaters, the values of the distribution coefficient range from 0.02 to 1.3 dm^3/g.

From the application of a Langmuir isotherm to the data, a density of surface sites of $(3.5 \pm 1.4)\cdot 10^{-7}$ mol/g is obtained, which is one order of magnitude lower than the value obtained by using the measured BET surface area of the magnetite samples.

The interaction between U(VI) and the surface of magnetite is reasonably well described by means of a surface complexation model involving the formation of two different surface complexes.

The study of the surface of the solid by means of XPS indicates that the initial attachment of U(VI) to magnetite may be followed by a much slower process of electronic transference which would imply the reduction of U(VI) to U(IV) and the subsequent oxidation of Fe(II) to Fe(III).

From the position of the U4f peak in experiment XPUI , it seems that the process of reduction of U(VI) does not take place at acidic pH, which can be due to the preferential release of the potential reductor (Fe(II)) observed under this conditions from the results of experiment XPIV.

Under the presence of carbonate, the shift of the peak of U4f to slightly lower energy values gives some indications on the possibility of the reduction process. Nevertheless, additional experiments should be performed to confirm this hypothesis.

The comparison of our data with some works found in the literature indicate that if the reduction process is occurring, it will be much slower than when sulphides such as galena or pyrite are used as substrates.

6 References

Allen G F, Crofts J, Curtis M T, Tucker P M, Chadwick D, Hampson P J, 1974a. X-Ray Photoelectron Spectroscopy of some uranium oxide phases. J C S Dalton Trans. 1296–1301.

Allen G F, Curtis M T, Hooper A J, Tucker P M, 1974b. X-Ray Photoelectron Spectroscopy of iron-oxygen systems. J C S Dalton Trans. 1525–1530.

Blesa M A, Figliolia N M, Maroto A J G, Regazzoni A E, 1983. The influence of temperature on the interface magnetite-aqueous electrolyte solution. J. Colloid Interface Science, 101 (2), 3713–3717.

Bruno J, Puigdomènech I, 1989. Validation of the SKBU1 uranium thermodynamic data base for its use in eochemical calculations with EQ3/6. Mat. Res. Soc. Symp. Proc. MRS, 127, 887–896.

Cui D, Eriksen T E, 1996. Reduction of Tc(VII) and Np(V) in solution by ferrous ion. A laboratory study of homogeneous and heterogeneous redox processes. SKB TR 96-03, Svensk Kärnbränslehantering AB.

Davis J A, Kent D B, 1990. Surface complexation modeling in aqueous geochemistry. In Mineral-Water Interface geochemistry (Hochella and White eds.) Min. Soc. Amer. Rev. In Mineralogy, 23, pp. 177–260.

de Pablo J, Casas I, Gimenez J. Martí V, Torrero M E, 1996. Solid surface evolution model to predict uranium release from unirradiated UO_2 and nuclear spent fuel dissolution under oxidizing conditions. J. Nucl. Mat. 232, 138–145.

El Aamrani F, Casas I, Martin C, Rovira M, de Pablo J, 1998. Effect of iron and canister corrosion products on the dissolution of UO_2. Proceedings of Spent Fuel Workshop 1998, Las Vegas, Nevada.

Fiodor J N, Bostick W D, Jarabek R J, Farrell J, 1998. Understanding the mechanism of uranium removal from groundwater by zero-valent iron using X-Ray Photoelectron Spectroscopy. Environ. Sci. Technol 32, 1466–1473.

Fujita T, Tsukamoto M, Ohe T, 1995. Modeling of Neptunium(V) sorption behavior onto iron-containing minerals. Mat. Res. Sco. Symp. Proc. 353 (part 2) 965–972.

Grambow B, Smailos E, Geckeis H, Müller R, Hentschel H, 1996. Sorption and reduction of Uranium(VI) on iron corrosion products under reducing saline conditions. Radiochim. Acta 74, 149–154.

Grenthe I, Fuger J, Konings R J M, Lemire R J, Muller, A B, Nguyen-Trung C, Wanner H, 1992. Chemical Thermodynamics. Vol 1. Chemical Thermodynamics of uranium, NEA (Wanner and Forest eds.) Elsevier.

Inagaki Y, Sakata H, Furuya H, Idemitsu K, Arima T, Banba T, Maeda T, Matsumoto S, Tamura Y, Kikkawa S, 1998. Effects of water redox conditions and presence of magnetite on leaching of Pu and Np from HLW glass. Mat. Res. Sco. Symp. Proc. 506, 177–184.

Jolivet J, Tronc E, 1988. Interface electron transfer in colloidal spinel iron oxide. Coversion of Fe_3O_4 to Fe_2O_3 in aqueous medium. J. Coll. Interface Sci. 125, 688–701.

McIntyre M R and Zetaruk D G, 1977. X-Ray Photoelectron Spectroscopy Studies of iron oxides. Anal. Chem. 49, 1521–1529.

Rodriguez E, El Aamrani F Z, Gimenez J, Casas I, Torrero M E, de Pablo J, Duro L, Hellmuth K H, 1998. Surface characterization of olivine-rock by X-Ray Photo-electron Spectroscopy (XPS). Leaching and uranium(VI)-sorption experiments. Mat. Res. Sco. Symp. Proc. 506, 321–327.

Sagert N H, Ho C H, 1989. The adsorption of Uranium (VI) onto magnetite sol. J. Colloid Interface Sci., 130 (1), 283–287.

Shoesmith D W, Sunder S, Bailey M G, Wallace G J, 1989. The corrosion of nuclear fuel (UO_2) in oxygenated solutions. Corros. Sci. 29, 1115–1128.

Smailos E, Schwarzkopf W, Kienzler B, Köster R, 1992. Corrosion of carbon-steeel container for heat-generating nuclear waste in brine environment relevant for a rock-salt repository. Mat. Res. Soc. Synp. Proc. 257, 399–406.

Stumm W, Morgan J J, 1996. Aquatic Chemistry 3rd Edition, Wiley Interscience.

Sverjensky D A, Sahai N, 1996. Theoretical prediction of single-site surface protonation equilibrium constants for oxides and silicates in water. Geochimica et Cosmochimica Acta 60, 3773–3797.

Tamura H, Katayama N, Furuichi R, 1996. Modeling of iron exchange reactions on metal oxides with the Frumkin Isotherm. I. Acid-Base and charge characteristics of MnO_2, TiO_2, Fe_3O_4 and Al_2O_3 surfaces and adsorption affinity of alkali metal ions. Environ. Sci. Tech. 30, 1198–1204.

Tewari P-H, McLean A W, 1971. Temperature dependence of point of zero charge of alumina and magnetite. J. Colloid Interface Sci., 40 (2), 267–272.

Wersin P, Hochella Jr M F, Persson P, Redden G, Leckie J O, Harris D W, 1994. Interaction between aqueous uranium(VI) and sulfide minerals: Spectroscopic evidence for sorption and reduction. Geochim. Cosmochim. Acta 58, 2829–2843.

White A F, Paterson M L, 1996. Reduction of aqueous transition metal species on the surface of Fe(II)-containing oxides. Geochim. Cosmochim. Acta 60, 3799–3814.

White A F, 1990. Heterogeneous electrochemical reactions associated with oxidation of ferrous oxide and silicates surfaces, In Mineral-Water Interface geochemistry (Hochella and White eds.) Min. Soc. Amer. Rev. In Mineralogy, 23, pp. 467–509.

Yoon R H, Salmn T, Donnay G, 1979. Predicting points of zero charge of oxides and hydroxides. J. Colloid Interface Science 70, 483–493.